

# A light Higgs particle explains physics mysteries

Stig Sundman  
Dragonvägen 12 A 5, FIN-00330 Helsinki, Finland

October 14, 2014

## Abstract

In a maximally simple model (MxSM), a straightforward interpretation of the Feynman diagrams for the elementary particles of the standard model (SM) leads to the prediction of a light, weakly interacting massive particle (WIMP), which is pictured by the same Feynman diagrams that describe the heavy Higgs boson observed in CERN's Large Hadron Collider (LHC). Like another WIMP, the neutrino, the light Higgs particle comes in three mass states associated with the electron, muon, and tauon, respectively. The particle may be thought of as a spin-0 photon, which because of mass conservation cannot be permanently emitted or absorbed by charged leptons or quarks. Consequently, it can be neither produced nor directly detected using standard laboratory instruments. Real light Higgs particles produced in the sun through neutrino-photon reactions manifest their presence in several ways. For instance, they heat the sun's corona, shorten the lifetimes of beta-decaying and electron-capturing radioactive isotopes, and contribute to the interstellar and intergalactic dark matter. Virtual light Higgs particles mediate a weak force, which may explain several phenomena that for a long time have puzzled physicists.

*Keywords:* Maximally simple model (MxSM); pure QED; light Higgs boson, WIMP.

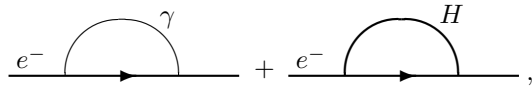
## Contents

<b>1</b>	<b>The spin-0 particle of the Feynman diagrams</b>	<b>3</b>
<b>2</b>	<b>Observations of real light Higgs particles</b>	<b>7</b>
2.1	The sun's hot corona . . . . .	8
2.2	The tritium endpoint anomaly . . . . .	8
2.3	Seasonal variations in radioactive half-lives . . . . .	9
2.4	The neutron lifetime discrepancy . . . . .	10
2.5	The lithium problem . . . . .	11
2.6	The galaxies' dark matter . . . . .	12
<b>3</b>	<b>Observations of virtual light Higgs particles</b>	<b>13</b>
3.1	The muon anomalous magnetic moment . . . . .	13
3.2	The proton's missing spin . . . . .	14
3.3	The nucleon's magnetic moment . . . . .	15
3.4	The proton radius . . . . .	15
3.5	The Hoyle state . . . . .	16
3.6	The flyby anomaly . . . . .	17
3.7	The Pioneer anomaly . . . . .	19
<b>4</b>	<b>Conclusions</b>	<b>19</b>

## 1 The spin-0 particle of the Feynman diagrams

The photon ( $\gamma$ ) is a massless neutral spin-1 boson, and the Higgs particle ( $H$ ) a massive neutral spin-0 boson. The photon is the carrier of the electromagnetic force, while the Higgs carries a weak force. In their interaction with matter — that is, with ordinary electrons ( $e^-$ ) and  $d$  and  $u$  quarks — they appear in identical-looking Feynman diagrams [1].

Considering in parallel the second-order mass contributions ( $\delta m^{(2)}$ ) to the electron from the photon and the Higgs,



one obtains from basic electroweak theory — for instance, following James Bjorkens and Sidney Drells classical text book [2] — the expression

$$m = m_0 + \delta m^{(2)}(\gamma) + \delta m^{(2)}(H) = m_0 + \frac{3\alpha}{2\pi} \left( \ln \frac{\Lambda}{m} \right) \left[ 1 + \frac{G_F m^2}{4\sqrt{2}\pi\alpha} \right] m, \quad (1)$$

for the renormalized mass  $m$  of the electron. In the equation,  $m_0$  is the bare mass of the electron,  $\alpha$  the fine-structure constant,  $G_F$  the Fermi coupling constant, and  $\Lambda$  a cut-off mass introduced to make the mathematics finite.

Ignoring other contributions to  $m$ , and relying on the observation that  $m_0 = 0$  in “pure QED” — which is also referred to as “finite QED,” or the “JBW hypothesis” after Kenneth Johnson, Marshal Baker, and Raymond Willey who developed the theory in the early 1960s [3] — one immediately gets from Eq. (1) the ratio

$$\frac{\delta m^{(2)}(H)}{\delta m^{(2)}(\gamma)} = \frac{G_F m^2}{4\sqrt{2}\pi\alpha} \quad (2)$$

between the two contributions to the mass of the electron.

Since the Higgs–electron diagrams exactly parallel the photon–electron diagrams, one may expect that the ratio between the Higgs and photon contributions to the electron mass will remain the same as in Eq. (2) when higher-order self-mass diagrams are included in the calculation. That is,  $\delta m(H)/\delta m(\gamma) = \delta m^{(2)}(H)/\delta m^{(2)}(\gamma)$  is expected to hold true.

Because Higgs and other corrections to the mass of the electron are small in comparison with the photon’s contribution to it, one may set  $\delta m(\gamma)$  equal to  $m$ , and obtain as a good approximation

$$\delta m(H) = \frac{G_F m^2}{4\sqrt{2}\pi\alpha} m. \quad (3)$$

Finally, resorting to the “principle of maximum simplicity” — a term coined by James Bjorken and Sidney Drell in 1965, when they discussed the role of simplicity as a guiding rule in the development of quantum field theory (QFT) [4]

— one may conjecture that the mass of the Higgs particle itself equals its contribution to the electron mass; that is,  $m_H$  may replace  $\delta m(H)$  in Eq. (3).

Using the values  $1/\alpha = 137.035\,999$  and (after restoring  $\hbar$  and  $c$ , which are customarily set equal to 1)  $G_F/(\hbar c)^3 = 1.166\,36 \times 10^{-5} \text{ GeV}^{-2}$ , one gets from Eq. (3) the relation

$$m_H = \frac{m^2}{11\,118.8 \text{ GeV}^2} m \quad (4)$$

between the mass  $m$  of the electron and the mass  $m_H$  of the light Higgs particle.

For the mass of a Higgs particle emitted by an ordinary electron (which possesses a mass of  $m_e = 0.510\,9989 \text{ MeV}$ ) and the heavier muon ( $m_\mu = 105.658\,37 \text{ MeV}$ ) and tauon ( $m_\tau = 1777 \text{ MeV}$ ), respectively, one obtains from Eq. (4)

$$\begin{aligned} m_{H_e} &= 12.0006 \text{ } \mu\text{eV}, \\ m_{H_\mu} &= 106.085 \text{ eV}, \\ m_{H_\tau} &= 0.505 \text{ MeV}. \end{aligned} \quad (5)$$

The self-energy,  $12.0006 \text{ } \mu\text{eV}$ , of the electron-type Higgs corresponds to the energy of a photon of frequency  $2.9017 \text{ GHz}$ .

In summary, a simple argument leads to the conclusion that the Higgs particle appears in four mass states: the heavy  $125 \text{ GeV}$  state observed at CERN, which creates the masses of the weakly interacting  $W^\pm$  and  $Z^0$  bosons, and three light states, which create small contributions to the masses of the light ( $e$ ), the heavy ( $\mu$ ), and the superheavy electron ( $\tau$ ), respectively.

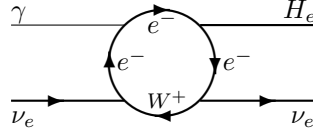
Note that that the Feynman diagrams, which form the hard core of the standard model (SM), do not specify in how many mass states elementary particles, such as the electron or Higgs, may appear.

In addition to the fact that the photon and Higgs mediate different forces (electromagnetic and weak, respectively) there is another important difference between them.

Because the photon carries zero mass, an electron can emit photons without recapturing them, and also absorb photons without reemitting them.

For the massive Higgs particle the situation is different. Electrons and quarks can neither convert the Higgs particle's weakly generated mass into energy, nor energy into weak mass. Therefore, a Higgs particle emitted by an electron or quark must be recaptured by the emitting particle within a time  $\Delta t$  determined by the Heisenberg uncertainty relation  $\Delta E \Delta t \geq \frac{1}{2} \hbar$ , which in this case may be replaced by  $\Delta E \Delta t = \hbar$  with  $\Delta E = m_H c^2$ . Similarly, a real Higgs particle absorbed by an electron or quark must be reemitted within the same time. The consequence is that real Higgs particles can be neither produced nor directly detected with standard laboratory instruments.

However, Higgs particles can be both created and annihilated in electroweak reactions involving the  $W$  particle. This is so because the charged  $W$  is capable of transforming weak Higgs mass into electromagnetic energy, and vice versa. Thus, in the sun,  $H_e$  particles are created in the process:

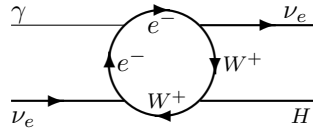


Beginning from the diagram's lower left vertex and following the vacuum-polarization (v-p) loop clockwise, one sees how an electron created by a neutrino absorbs an incoming photon and emits an electron-type Higgs particle, after which it emits a neutrino at the same time as it transforms into a  $W^-$  particle, which travels backward in time and finally completes the v-p loop by returning to the vertex in which the electron was created.

Looking at the diagram in this way — not as an  $e^- - W^+$  pair-production process, but as an  $e^- - W^-$  loop — demonstrates that the  $W^+$  is equivalent to a  $W^-$  particle moving backward in time. That is, the left-pointing arrow in the diagram means that the  $W^-$  is taken to be particle and  $W^+$  its antiparticle.

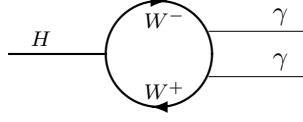
Similar diagrams describe  $H_\mu$  and  $H_\tau$  production via  $\mu^- - W^-$  and  $\tau^- - W^-$  loops, respectively. Eq. (1) shows that the probability of the light ( $e$ ), heavy ( $\mu$ ), or superheavy electron ( $\tau$ ) emitting a Higgs particle is independent of the Higgs mass and grows with the electron mass ( $m$ ).

In an alternative process, neutrinos of any type ( $\nu_e$ ,  $\nu_\mu$ , or  $\nu_\tau$ ) may create Higgs particles of any type:



In this case, the probability of the  $W$  particle emitting a Higgs particle is independent of the electron mass and grows with the Higgs mass (see Eq. (7) below). Note that the masses  $m_{H_\tau} = 0.505$  MeV and  $m_e = 0.511$  MeV almost coincide, which suggests that about as much  $H_\tau$  particles are created through this process as there are  $H_e$  particles produced in the first-mentioned process.

The Higgs particle is unstable, and its annihilation described by the Feynman diagram



in which  $H$  may be any one of the three light Higgs bosons (with mass  $m_{H_e} = 12.0006 \mu\text{eV}$ ,  $m_{H_\mu} = 106.085 \text{ eV}$ , and  $m_{H_\tau} = 0.505 \text{ MeV}$ , respectively) or the heavy Higgs (with mass  $M_H \approx 125 \text{ GeV}$ ).

For the same reason that a real electron cannot absorb a Higgs particle without reemitting it, the particles in the electron or quark loops that appear in the Higgs propagator are unable to transform the weak mass of the Higgs into electromagnetic energy. Therefore, in lowest order, the only way in which a Higgs particle may spontaneously annihilate is through the virtual  $W$  loop shown in the above figure.

The lifetimes of the three light Higgs particles are

$$\begin{aligned}\tau_{H_e} &= 2.7 \times 10^{22} \text{ yr}, \\ \tau_{H_\mu} &= 39.45 \text{ yr}, \\ \tau_{H_\tau} &= 1.15 \times 10^{-2} \text{ s}.\end{aligned}\tag{6}$$

The values follow from the decay width presented in a text book in particle physics and cosmology [5].

For a Higgs particle decaying through a  $W$  loop, the decay width is

$$\Gamma(H \rightarrow \gamma\gamma) = \frac{G_F m_H^3}{8\sqrt{2}\pi} \left(\frac{\alpha}{\pi}\right)^2 |I'|^2\tag{7}$$

with  $|I'|^2 \simeq \frac{1}{4}$ . After restoring  $\hbar$  and  $c$ , which are set equal to 1 in Eq. (7), and using  $G_F(\hbar c)^{-3} = 1.166\ 37 \times 10^{-5} \text{ GeV}^{-2}$ ,  $m_{H_e} c^2 = 12.0006 \times 10^{-15} \text{ GeV} = 12.0006 \times 10^{-6} \text{ eV}$ , and  $\alpha^{-1} = 137.036$ , one obtains the value

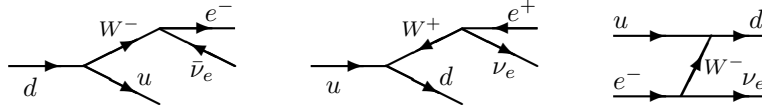
$$\Gamma(H_e \rightarrow \gamma\gamma) = \frac{G_F(\hbar c)^{-3} (m_{H_e} c^2)^2}{32\sqrt{2}\pi} \left(\frac{\alpha}{\pi}\right)^2 m_{H_e} c^2 = 7.6500 \times 10^{-46} \text{ eV}\tag{8}$$

for the decay width of the  $H_e$  particle. The corresponding lifetime is  $\tau_{H_e} = \hbar/\Gamma(H_e \rightarrow \gamma\gamma)$ , which follows from the Heisenberg uncertainty relation  $\Delta E \times \Delta t = \hbar$  with  $\Delta E = \Gamma$  and  $\Delta t = \tau$ . Using  $\hbar = 6.582\ 119 \times 10^{-16} \text{ eV s}$ , one gets  $\tau_{H_e} = 8.604 \times 10^{29} \text{ s} = 2.7 \times 10^{22} \text{ yr}$  for the lifetime of the  $H_e$  particle. The  $H_\mu$  and  $H_\tau$  lifetimes are obtained via division of  $\tau_{H_e}$  by  $(m_{H_\mu}/m_{H_e})^3$  and  $(m_{H_\tau}/m_{H_e})^3$ , respectively.

Since its lifetime is about  $10^{12}$  times the estimated age of the universe, the lightest Higgs particle may be regarded as stable. Therefore,  $H_e$  particles produced in stars accumulate in galaxies in the form of dark matter. Note that the Higgs particle is a weakly interacting massive particle (WIMP).

## 2 Observations of real light Higgs particles

In addition to decaying spontaneously, Higgs particles may be destroyed in beta-decay and electron-capture processes, which normally proceed in the manner shown in the figure:

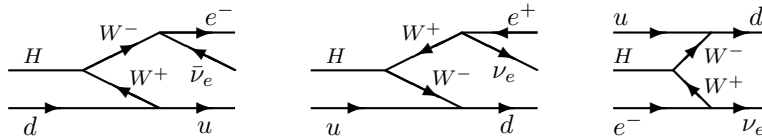


The left diagram illustrates  $\beta^-$  decay through which a neutron ( $udd$ ) transforms into a proton ( $uud$ ), an electron, and an antineutrino.

The diagram in the middle illustrates  $\beta^+$  decay through which a proton transforms into a neutron, an antielectron (i.e., a positron), and a neutrino.

The diagram to the right shows electron capture — the process through which a proton transforms into a neutron by capturing an electron and emitting a neutrino. In the figure, a  $W^-$  particle emitted by the electron is absorbed by a  $u$  quark. Alternatively, one of the proton's two  $u$  quarks may emit a  $W^+$  particle that is absorbed by the electron being captured.

In all three types of weak decay, a Higgs particle may appear and trigger the reaction, thereby accelerating the decay rate:



In these Higgs-capture diagrams,  $H$  may in principle be any one of the four Higgs particles, but in practice only the two lightest of them,  $H_e$  and  $H_\mu$ , live long enough to show up in laboratories on the earth.

In the sun, as well as in the earth,  $H_e$  and  $H_\mu$  behave differently. Since  $H_e$  interacts with electrons, it resembles an ordinary photon — one might call it the “Higgs photon” or “spinless photon”. The atom's electron shell tends to shield the nucleus from being hit by Higgs photons. Still, because the spin-0 (or polarization-free)  $H_e$  interacts much more weakly with the electron than the photon does, it will occasionally penetrate the shell and collide with a quark in the atom's nucleus. Consequently, the spinless photon may travel long distances in a more or less straight line and only rarely change direction through elastic collisions with quarks.

The result is that  $H_e$  particles created in the corona by neutrinos produced in the sun's core rapidly leak out from the corona and hit the earth. Therefore, fluctuations in solar neutrino production are almost instantly accompanied by variations in the number of  $H_e$  particles arriving at the earth.

Because of the long mean free path of the particles, they rapidly spread through the earth, which means that a sudden increase or decrease in solar

neutrino production might be observed even at night. Another effect of their long mean free path is that the  $H_e$  particles rapidly leak out into space.

The  $H_\mu$  particles, which interact with quarks and muons but not with ordinary electrons, behave in much the same way as neutrons in the moderator of a nuclear reactor. Because they constantly change direction of motion in their frequent collisions with quarks, they spread slowly. This property, in combination with their lifetime of 39.45 yr, enables them to accumulate in large numbers in the earth.

## 2.1 The sun's hot corona

The sun's atmosphere consists of the photosphere hundreds of kilometers thick with an average temperature  $T$  of 5780 K, the chromosphere about 10 000 km thick with  $T$  rising from about 4000 K to about 50 000 K, and the corona with  $T$  reaching about 2 million K at a height of some 75 000 km [6].

The high temperature of the corona has mystified astrophysicists, and no convincing explanation for it has been found.

In want of a simple explanation, it has been suggested that the corona's high temperature is caused by hypothetical so-called nanoflares, which are too small to be individually detected, and with an underlying mechanism that is not known [7].

The presence of light Higgs particles solves the mystery. Solar neutrinos created in boron decay,  ${}^8_5\text{B} \rightarrow {}^8_4\text{Be}^* + e^+ + \nu_e$ , acquire energies approaching 14 MeV [8]. Consequently,  $\tau$ -type Higgs particles are produced in large numbers in the corona. Living about 0.01 seconds, the  $H_\tau$  particles rapidly annihilate into pairs of photons. With  $E = m_{H_\tau}c^2 = 0.505$  MeV and  $T = 2T_\gamma$ , one obtains from the relation  $E = kT$ , where  $k$  is the Boltzmann constant,  $T_\gamma = 0.5 \times 0.505 \text{ MeV} / 8.617 \times 10^{-5} \text{ eV/K} = 2.9$  GK. This means that the initial temperature of the photons is a thousand times higher than the maximum temperature of the corona.

p. 6  
p. 4

Naturally, the local temperature of the corona depends on its matter density and how fast old matter is replaced with new matter brought by large solar flares.

It should be a fairly easy task to calculate the amount of  $H_\tau$  particles produced in the sun's atmosphere, and estimate how much they heat the corona.

## 2.2 The tritium endpoint anomaly

Beta decay of tritium means that a radioactive hydrogen atom with one proton and two neutrons in its nucleus ( ${}^3_1\text{H}$ , or tritium) decays into a helium-3 atom ( ${}^3_2\text{He}$ ) with two protons and one neutron in its nucleus at the same time as a beta particle ( $e^-$ ) and an antineutrino ( $\bar{\nu}_e$ ) are emitted:  ${}^3_1\text{H} \rightarrow {}^3_2\text{He} + e^- + \bar{\nu}_e$ .

When physicists began to suspect that the mass of the neutrino is not zero, which it originally was assumed to be, they tried to determine the mass  $m_{\nu_e}$  of the electron neutrino by measuring the energy of the outgoing electron and comparing it to the energy known to be released in the decay. A negative

difference even in the limit of zero kinetic energy ( $v_{\nu_e} = 0$ ) of the neutrino would indicate that the neutrino has nonzero mass.

Against all expectations, the difference proved to be neither negative nor zero, but positive. No explanation was found for this phenomenon, which was dubbed “the tritium endpoint anomaly.” (The possibility that the excess energy might derive from neutrinos captured by the tritium nucleus was soon ruled out.)

Another puzzling observation was that the anomalous energy difference was not constant, but changed randomly from one measurement to another. This finding suggests that the effect is largely caused by the lightest Higgs particle (the spinless photon  $H_e$ ), since the number density of the heavier  $H_\mu$  in the earth is expected to vary rather slowly, reaching its maximum in January when, at perihelion, the earth is nearest to the sun, and its minimum in July when, at aphelion, the earth is farthest from the sun.

### 2.3 Seasonal variations in radioactive half-lives

For a long time, it has been taken as an established fact that radioactive decay rates are constant. However, in recent years the validity of this assumption has been questioned. A number of observations indicate that the half-lives of beta-decaying radionuclides exhibit seasonal variations [9, 10]. It has been suggested that the influence could arise from some flavor of solar neutrinos or through objects called “neutrellos,” which behave in some ways like neutrinos [11]. An obvious candidate for the neutrello particle is the Higgs boson in the form of  $H_e$  and  $H_\mu$  particles.

According to an article written in 2008 [12], the decay rate of a sample of chlorine-36, which has a half-life of about 300 000 years, “had rates of decay that varied with the seasons, by about 0.3 percent.”

Assuming that the observed effect really exists, and that the actual variation is 0.2 %, a short calculation shows that the total decay-accelerating effect of the neutrellos, or light Higgs particles, should be about 3 %.

At perihelion on about 3 January, the earth is approximately  $r = 147$  million km from the sun, and at aphelion on about 3 July, some  $r = 152$  million km from it. The number of solar Higgs particles arriving from the sun should be proportional to  $1/r^2$ . That is, there should be a variation of almost seven percent ( $n \propto 1/r^2$  gives  $dn/n = -2dr/r = -10/150 = -1/15$ ) in the number of Higgs particles reaching the earth. Assuming for simplicity that the seasonal variation in the decay rate of Cl-36 is 0.2 percent, one finds (solving  $0.2/x = -dn/n = 1/15$ ) that the flux of Higgs particles from the sun should cause a total increase in decay rates of 3.0 percent.

A way of verifying that neutrellos accumulated in the earth are responsible for the decay-accelerating effect could be to place a radioactive sample on board a spacecraft and measure how the decay rate varies with increasing distance from the earth.

## 2.4 The neutron lifetime discrepancy

The neutron is a beta-decaying particle ( $n \rightarrow p + e^- + \bar{\nu}_e$ ) with assumingly constant half-life. Still, measurements of the neutron's lifetime ( $\tau_n$ ) using the beam method and the bottle method, respectively give different results. The difference is reported to be  $\Delta\tau_n = \tau_n^{\text{beam}} - \tau_n^{\text{bottle}} = (888.0 \pm 2.1) \text{ s} - (879.6 \pm 0.8) \text{ s} = (8.4 \pm 2.2) \text{ s}$ , which implies a  $3.8\sigma$  discrepancy between the two results [13].

Beam experiments are performed in laboratories at room temperature. In bottle experiments ultracold neutrons (UCNs) are used. Consequently, in laboratories performing bottle experiments, there is cold matter present. For instance, liquid deuterium may be used to first cool the neutrons from room temperature to about 25 K. This fact suggests that cold  $H_\mu$  particles present in bottle experiments are responsible for the accelerated decay of the neutrons.

At room temperature (20 °C = 293.15 K), the most probable speed of the muon-type Higgs is about 6500 km/s.

The most probable speed of a thermal particle of mass  $m$  is  $v = \sqrt{2kT/m}$ , where  $k$  is the Boltzmann constant. For a thermal neutron of mass  $m_n = 939.565 \text{ MeV}/c^2$  at a temperature of 20 °C = 293.15 K, one obtains  $v_n^2 = 2 \times 8.617 \times 10^{-5} \text{ eV K}^{-1} \times 293.15 \text{ K} / 939.565 \times 10^6 \text{ eV}/c^2 = 53.771 \times 10^{-12} c^2$ . Consequently,  $v_n = 7.3329 \times 10^{-6} c = 7.3329 \times 10^{-6} \times 299\,792\,458 \text{ m/s} = 2198 \text{ m/s} = 2.2 \text{ km/s}$ .

Correspondingly, the most probable speed of the  $H_\mu$  particle is, with  $m_n = 939.565 \text{ MeV}$  and  $m_{H_\mu} = 106.085 \text{ eV}$ ,  $(m_n/m_{H_\mu})^{1/2} = 2976$  times higher than  $v_n$ , or  $v_{H_\mu} = 6\,541\,300 \text{ m/s} = 6541 \text{ km/s}$ .

One may expect that the slower the Higgs particles move, the greater is the probability that they will trigger the decay of free neutrons or weakly decaying radionuclides they happen to collide with.

A simple argument suggests that (at least for temperatures not very close to absolute zero) the  $H_\mu$  particle's accelerating effect on decay rates should be inversely proportional to its temperature. Imagining the quarks, which may be taken to move at the speed of light, and the Higgs as classical point particles, one may conclude that the longer it takes for the  $H_\mu$  particle to traverse a neutron, the higher is the probability that it will collide with a relativistic quark orbiting inside the neutron.

In the same time ( $t = 2r/v$ ) as the  $H_\mu$  particle with speed  $v$  traverses a neutron with radius  $r$ , a quark moving in a circular orbit having the same radius will circle the neutron  $N = (2r/v)/(2\pi r/c) = c/\pi v$  times. With  $v = 6500 \text{ km/s}$ , one obtains  $N = 300\,000/6500\pi = 15$ .

Liquid nitrogen has a temperature of about  $T = -196 \text{ °C} = 77 \text{ K}$ , and liquid helium  $T = -269 \text{ °C} = 4 \text{ K}$ . This means that in an environment cooled to the temperature of liquid nitrogen, the decay-accelerating effect of the  $H_\mu$  particle should be  $293/77 = 3.8$  times higher than at room temperature. Similarly, at an ambient temperature equal to the temperature of liquid helium, the factor by which the decay rate is enhanced should be  $293/4 = 73$ .

To what extent  $H_\mu$  particles are moderated, or cooled, before they hit the UCNs trapped in the bottle depends on how much cold matter there is in the laboratory and how far away from the bottle it is situated.

Fortunately, there is no need to do very advanced calculations and experiments in order to study the connection between the half-life of a beta-decaying nuclide and the temperature of the ambient structures. For example, in a low-cost experiment one could put a radioactive sample (such as chlorine-36 in the form of common salt, NaCl) in the middle of a well-insulated freezer or chamber in which the temperature is held at 77 K by vessels filled with liquid nitrogen placed in the corners or along the walls of the freezer.

After measuring the sample's decay rate during a day or two, one should build a moderating wall around the sample using bricks of a suitable material, such as lead, already cooled to 77 K in liquid nitrogen. After again measuring the decay rate during a couple of days, one should make the wall thicker using more cold bricks. The process should be repeated until the freezer is filled with moderating material. Finally, one should measure the decay rate during a longer period, then remove all bricks and repeat the measurement during an equally long period.

From the experimental data, it should now be possible to estimate how much moderating material efficient cooling of thermal  $H_\mu$  particles requires, and thereby determine the mean free path of the particles.

If the mean free path of the  $H_\mu$  particle is long, the suggested experiment may not produce decisive evidence for the existence of thermal  $H_\mu$  particles. Nor can the neutron lifetime discrepancy be explained by the presence of "cryonic matter" in the laboratories. In this case, a better experiment might be to simultaneously measure the decay rate in a hot and in a cold environment, such as on the slope of a recently active volcano, where the ground is still hot, and on the top of a glacier, respectively.

Identical samples and measuring equipment should be used, and the samples interchanged at regular intervals. In both cases, the apparatus might be installed in an air-conditioned car, in which temperature and air humidity are kept constant.

For instance, a difference between +30 °C and 0 °C means a relative temperature difference of about ten percent (30 K divided by 293 K). Thus, assuming that the  $H_\mu$  particles are responsible for the 3.0 % increase in decay rates suggested in Section 2.3, the variation observed in the experiment should be about 0.3 %.

Note that seasonal variations in decay rates are expected to be largest in the Northern Hemisphere, where the low winter temperature tends to accelerate the decay rate at the same time as the earth is nearest to the sun.

## 2.5 The lithium problem

In the hot interior of stars, lithium is burned to helium through fusion with a proton ( ${}^7_3\text{Li} + p \rightarrow {}^8_4\text{Be} + 17.3 \text{ MeV}$ ) followed by fission of the resulting beryllium nucleus ( ${}^8_4\text{Be} \rightarrow {}^4_2\text{He} + {}^4_2\text{He} + 92 \text{ keV}$ ). Proton–lithium fusion requires a temperature of approximately  $2 \times 10^6 \text{ K}$ , which is less than the  $2.5 \times 10^6 \text{ K}$  necessary for hydrogen fusion. Only protons possessing energies much higher

than their average energy are able to overcome the Coulomb barrier and fuse with lithium nuclei.

With a lifetime of about  $7 \times 10^{-17}$  s, the beryllium-8 nucleus almost instantly splits into two helium nuclei (or alpha particles), each one carrying about 8.6 MeV of kinetic energy.

The amount of lithium-7 believed to have been created in the primordial nucleosynthesis matches the amount observed in the Small Magellanic Cloud [14].

However, in the atmospheres of old, so-called galactic halo stars, there is about one fourth as much lithium-7 as predicted [14].

A possible explanation for this mismatch between theory and observation is supplied by the light Higgs particle, or neutrello, which suggests a mechanism through which solar neutrinos may cause lithium depletion. That is, in a collision with a proton, a high-energy neutrello may heat the proton to a temperature that enables it to fuse with a lithium-7 nucleus.

An experiment performed in 1932 demonstrated that, for a proton to be able to overcome (or tunnel through) the Coulomb barrier and fuse with a lithium-7 nucleus, it requires an energy of about 0.1 MeV [15]. This energy is several hundred times higher than the energy  $E = kT = 170$  eV corresponding to the temperature  $T = 2 \times 10^6$  K. (The average kinetic energy of a *thermal neutron* [16] is  $\frac{3}{2}kT$ , its most probable kinetic energy is  $\frac{1}{2}kT$ , and its most probable speed  $v = (2kT/m)^{1/2}$ ; that is, a thermal particle with kinetic energy  $\frac{1}{2}mv^2 = kT$  moves with the most probable speed.)

Solar neutrinos created in boron decay acquire energies approaching 14 MeV. In the  $\nu_e \gamma \rightarrow \nu_e H_e$  process, the neutrino may give over most of its energy to the neutrello it creates from a photon. For simplicity, assume that the neutrello gets an energy of 9.38 MeV, which is one percent of the proton's rest energy. According to Eq. (9) below, it means that  $\Delta E/E = 0.02$ . In other words, the proton may acquire two percent of the neutrello's energy, or 0.19 MeV, which is more than it needs to fuse with a lithium nucleus. It follows that a single neutrello with an initial energy about or above 10 MeV may heat dozens of protons to 0.1 MeV. p. 8

The massless photon's energy  $E$  is connected to its momentum  $p$  via the relation  $E = pc$ . The same relation holds approximately for a relativistic particle with energy  $E \gg mc^2$ . Conservation of momentum in the light neutrello's elastic head-on collision with a proton at rest means that the neutrello reverses its direction and that, consequently,  $p = -(p - \Delta p) + Mv$ , where  $M$  is the mass of the proton and  $v$  its speed. For the light neutrello (compare with a light ping-pong ball hitting a heavy solid iron ball), its loss of momentum,  $\Delta p$ , may be ignored. Thus,  $p = -p + Mv$ , or  $Mv = 2p = 2E/c$ . That is, the maximum energy passed to the proton is  $\Delta E = \frac{1}{2}Mv^2 = \frac{1}{2}(Mv)^2/M = 2p^2/M = 2E^2/Mc^2$ , and

$$\Delta E/E = 2E/Mc^2. \quad (9)$$

## 2.6 The galaxies' dark matter

Observations of the motion of stars in the Milky Way and other galaxies suggest that the universe contains considerable amounts of so-called missing mass, or

dark energy. Many candidates for the missing mass have been put forward. They include weakly interacting massive particles (WIMPs), to which belong the neutrino together with a number of hypothetical, so-called exotic particles that are not part of the standard model.

Also the standard model's Higgs particle is a WIMP. However, being unstable, it has not been included in the list of dark-matter candidates. Now, with a lifetime of  $2.7 \times 10^{22}$  yr, the predicted  $H_e$  particle is practically stable and will, consequently, contribute to the universe's dark matter. p. 6

It should be a straightforward task to calculate how much  $H_e$  particles are produced, and estimate their effect on the motion of stars in galaxies.

### 3 Observations of virtual light Higgs particles

In the same way as virtual photons mediate the electromagnetic force, virtual Higgs particles mediate a weak force. As a result, the light virtual Higgs particles manifest their presence in many ways.

#### 3.1 The muon anomalous magnetic moment

Convincing evidence for the existence of the  $H_\mu$  particle is provided by the E821 muon ( $g - 2$ ) experiment at Brookhaven [17], which yielded the value [18]

$$a_\mu^{\text{exp}} = 0.001\,165\,920\,91(63) \quad (10)$$

for the muon's anomalous magnetic moment  $a_\mu$  (equal to  $g_\mu - 2$  divided by 2).

If the Higgs particle ( $H_\mu$ ) appearing in the diagram that describes its contribution to  $a_\mu$  is much heavier than the muon itself (for instance, if  $H_\mu$  is identical to the 125 GeV boson observed at CERN), its contribution to  $a_\mu$  is vanishingly small. In this case, one obtains for the sum of the standard model's contributions to  $a_\mu$  the theoretical value

$$a_\mu^{\text{th}}(\text{SM}) = 0.001\,165\,917\,78(61) \quad (m_{H_\mu} \gg m_\mu). \quad (11)$$

It means that the difference between the experimental and theoretical values is

$$a_\mu^{\text{exp}} - a_\mu^{\text{th}} = +0.000\,000\,003\,13(88) \quad (m_{H_\mu} \gg m_\mu), \quad (12)$$

implying a discrepancy of  $313/88 = 3.5$  times the combined experimental and theoretical uncertainties (which are added in quadrature:  $63^2 + 61^2 = 88^2$ ).

On the other hand, if the Higgs mass is much smaller than the muon mass, its contribution to the anomalous magnetic moment of the muon is

$$a_\mu(H_\mu) = \frac{3G_F m_\mu^2}{8\sqrt{2}\pi^2} = 0.000\,000\,003\,50 \quad (m_{H_\mu} \ll m_\mu), \quad (13)$$

giving a total theoretical value of

$$a_\mu^{\text{th}}(\text{SM}) = 0.001\,165\,921\,28(61) \quad (m_{H_\mu} \ll m_\mu), \quad (14)$$

which means that the difference now is

$$a_\mu^{\text{exp}} - a_\mu^{\text{th}} = -0.000\,000\,000\,37(88) \quad (m_{H_\mu} \ll m_\mu). \quad (15)$$

Being well within the margin of error, the result indicates good agreement between the theoretically predicted and experimentally measured values. Consequently, the Brookhaven experiment convincingly demonstrates that the Higgs particle contributing to  $a_\mu$  is lighter than the muon; that is,  $m_{H_\mu} < m_\mu = 105.658$  MeV.

The anomalous magnetic moment of the electron,  $a_e$ , has been experimentally determined with a precision about 2000 times higher than that of  $a_\mu$ . The value obtained is [19]

$$a_e^{\text{exp}} = 0.001\,159\,652\,180\,73(28). \quad (16)$$

However, the  $H_e$  contribution to the electron anomalous moment,

$$a_e(H_e) = \frac{3G_F m_e^2}{8\sqrt{2}\pi^2} = 0.000\,000\,000\,000\,08 \quad (m_{H_e} \ll m_e), \quad (17)$$

is  $(m_\mu/m_e)^2$ , or about 40 000 times smaller than  $a_\mu(H_\mu)$ . Therefore, in spite of the high precision achieved in the electron ( $g - 2$ ) experiment, the result is not precise enough to provide any new information about the value of  $m_{H_e}$ .

### 3.2 The proton's missing spin

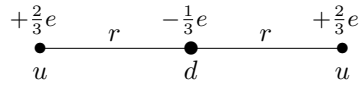
A comparison between the Higgs and photon Feynman diagrams suggests that the Higgs-mediated force between two charged particles is repulsive, independent of the signs of the charges (whereas the photon-mediated electromagnetic force is attractive or repulsive depending on whether the charges are of opposite or equal sign, respectively).

The fact that no repulsive static force attributable to the Higgs has been observed means that the Higgs-mediated force is of purely dynamic nature, possibly resembling the photon-mediated magnetic force.

In nuclear physics, there are a number of puzzling observations, which might be explained by the existence of a very light Higgs particle that produces a force of sufficiently long range to affect the behavior of the constituent particles (the down and up quarks) of the nucleons. One of these effects is “the proton’s missing spin.”

The proton’s spin is the sum of the orbital and spin angular momenta of its constituent particles (quarks and gluons). However, experiments indicate a gap between the proton’s spin angular momentum of  $\frac{1}{2}\hbar$  and the sum of its component particles’ theoretically estimated orbital angular momenta and observed spin angular momenta [20]. A Higgs force affecting the dynamics of the quarks might explain the discrepancy.

Asymptotic freedom implies that the strong force, which glues quarks together, vanishes for  $r \ll r_p$ , where  $r$  is the distance between the quarks and  $r_p$  the proton radius. The figure shows the quarks of the proton positioned on a common line with the down quark of fractional charge  $-\frac{1}{3}e$  at the center:



The electric force between one of the up quarks and the down quark is attractive and proportional to  $-(+\frac{2}{3}e)(-\frac{1}{3}e)r^{-2} = +\frac{2}{9}e^2r^{-2}$ , where  $e$  is the unit charge. The corresponding force between the two up quarks is repulsive and proportional to  $-(+\frac{2}{3}e)^2(2r)^{-2} = -\frac{1}{9}e^2r^{-2}$ . The positive sum,  $+\frac{2}{9}e^2r^{-2} - \frac{1}{9}e^2r^{-2} = +\frac{1}{9}e^2r^{-2}$ , implies that there is a net inward force acting on the quarks even when  $r$  is small and the strong force negligible. Consequently, the three quarks tend to stick closely together at the center of the proton, which means that their orbital angular momenta are small.

The situation changes radically if a repulsive Higgs force outweighs the attractive electromagnetic force and causes the quarks to move in orbits as wide as allowed by the strong force (which, like the force of a rubber band, increases with increasing  $r$ ). Therefore, if virtual lightweight Higgs particles are present, the angular momenta of the quarks might be considerably larger than they would be if the Higgs particles are absent.

Consequently, the existence of light scalar Higgs bosons provides a simple explanation for the proton's missing-spin mystery within the framework of SM.

### 3.3 The nucleon's magnetic moment

The theoretically predicted values for the magnetic moments of the proton, neutron, and other hadrons tend to be considerably smaller than the experimentally observed values [21].

The same effect that explains the "proton spin crisis" — why the sum of the quarks' theoretically calculated spatial angular momenta, the experimentally determined quark spin angular momenta, and the estimated net glue polarization is less than the proton's spin — should explain why the magnetic moments of hadrons are larger than theoretical considerations suggest they should be.

### 3.4 The proton radius

Another problem in nuclear physics is that measurements of the proton radius using muonic hydrogen (where the electron that orbits the proton is replaced by a muon) and ordinary hydrogen yield nonmatching results:  $r_p = 0.841\ 84(67)$  fm and  $0.8768(69)$  fm, respectively [22].

The straightforward explanation for the difference,  $0.035(7)$  fm, is that the light muon-type Higgs, whose existence the Brookhaven muon  $g-2$  experiment

convincingly demonstrates (see Section 3.1), causes a repulsive force between the quarks of the proton and the muon orbiting it.

The “Bohr radius” of the hydrogen atom is  $a_0 = 52\,918$  fm. For a proton circled by a muon, the corresponding radius is smaller by a factor of  $m_\mu/m_e$ . That is,  $a = a_0/206.768 = 256$  fm for muonic hydrogen atoms.

For the repulsive force to be of sufficiently long range, the force-mediating gauge particle must be light. The maximum lifetime of a virtual particle is determined by the Heisenberg uncertainty relation  $\Delta t \Delta E = \hbar$ . Using the value for  $m_{H_\mu}$  given in Eq. (5), one obtains a lifetime of  $\Delta t = \hbar/m_{H_\mu} c^2 = 6.582 \times 10^{-16}$  eV s / 106.085 eV =  $6.2 \times 10^{-18}$  s. The distance a particle with speed near  $c$  may travel in this time should give an indication of the maximum reach of the force it mediates. For  $H_\mu$ , it is  $c\Delta t = 2.998 \times 10^8$  m s $^{-1} \times 6.2 \times 10^{-18}$  s = 1.86 nm, which is considerably larger than the radius  $a$  of the atom of muonic hydrogen.

For the heaviest ( $H_\tau$ ) of the three light spinless particles, one similarly obtains  $c\Delta t = 390$  fm, which means that the force it mediates is of sufficient reach for it to play a crucial role in atomic nuclei (compare 390 fm with the value 0.8768(69) fm of the proton radius).

### 3.5 The Hoyle state

In a normal star — such as the sun — four hydrogen nuclei,  ${}^1_1\text{H}$ , fuse into a helium nucleus, or alpha particle,  ${}^4_2\text{He}$ . When the star exhausts its hydrogen fuel, it expands to a red giant, in which two alpha particles combine to form an unstable  ${}^8_4\text{Be}$  isotope (the stable isotope of beryllium is  ${}^9_4\text{Be}$ ). Fusion of a  ${}^8_4\text{Be}$  and a  ${}^4_2\text{He}$  nucleus, in turn, produces a stable  ${}^{12}_6\text{C}$  nucleus.

Because of the short lifetimes of the various beryllium-8 states — about or below  $10^{-16}$  s — a beryllium and a helium nucleus will in general not fuse directly into a ground-state carbon nucleus. Instead, creation of carbon in red giants proceeds through an intermediate, short-lived excited state of carbon-12 — the so-called Hoyle state.

A recently performed *ab initio* lattice calculation [23] of the ground and Hoyle states of carbon-12 shows that there is a bent-arm configuration associated with the Hoyle state, while a compact triangular configuration is associated with the ground state:



The figure suggests that a repulsive dynamic force of longer range than the attractive strong force may be active when the three alpha particles rapidly (within beryllium-8’s lifetime of about or less than  $10^{-16}$  s) form an elongated Hoyle state instead of a more compact state.

The strong force attempts to gather the alpha particles in a compact configuration. This process is counteracted by the repulsive electrostatic force between the positively charged alpha particles. However, the action of these two well-known, essentially static forces cannot explain the details of the Hoyle state, which is found to be of a highly dynamic nature; for instance, evidence is found for a “low-lying spin-2 excitation of the Hoyle state” [23].

Consequently, the assumption of an additional, dynamically generated repulsive force is needed to account for the properties of the Hoyle state.

### 3.6 The flyby anomaly

The so-called flyby anomaly is an unexpected change in velocity of spacecraft headed for distant regions of the solar system when they pass near the earth to change direction and increase or decrease their speed. The strength of the effect appears to vary randomly from spacecraft to spacecraft.

An explanation for the effect could be that virtual  $H_e$  particles in the photon propagator cause radio signals with frequencies near 2.9017 GHz to be “anomalously” delayed when they traverse the ionosphere and the Van Allen belts. p. 4

The “Higgs delay” will not only affect distance measurements, but also give rise to a transverse motion of the signal.

The ionosphere follows the earth’s rotation around its axis. The Van Allen belts form a doughnut-shaped zone symmetric about the axis connecting the north and south magnetic poles. Since this axis is oblique in relation to the earth’s axis of rotation, the Van Allen belts are seen from the spacecraft to be rocking up and down with a period of 24 hours. Consequently, in their passage through the Van Allen belts and the ionosphere, the radio signal’s photons will drift sideways together with the particles (free electrons in the ionosphere and free protons and electrons in the Van Allen belts), which absorb and reemit them. The strength of the effect depends on the direction from which the spacecraft approaches the earth, and varies with the hour.

A photon traveling through empty space oscillates between various states. In addition to forming a single-photon state, it may form a virtual particle pair consisting of any charged elementary particle and its antiparticle (a so-called polarization loop). Examples:



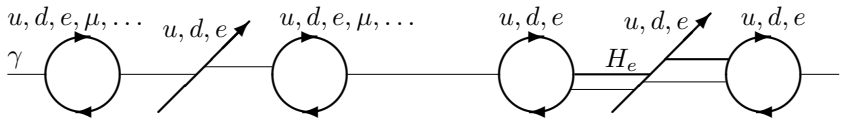
Note that left-pointing arrows are used to indicate that antiparticles, such as  $e^+$  and  $\bar{u}$  in the picture, may be regarded as particles moving backward in time. Also, note that the virtual massive particles appearing in the photon propagator

do not slow down the speed of a free photon, which in vacuum travels at the speed of light,  $c$ .

Through mediation of polarization loops, the photon may momentarily transform into a photon triplet (left) or a Higgs–photon pair (right) but, according to Furry’s theorem, not a pair of photons:



The lifetime of the Higgs–photon state depends on the ratio between the photon’s energy ( $E_\gamma$ ) and the Higgs particle’s rest energy ( $m_H c^2$ ). The closer these energies are to each other, the longer the lifetime of the Higgs–photon pair will be. And the longer it exists, the higher the probability of the pair hitting an electron or quark in its path will be (right half of the figure):



A polarization loop appearing in the photon propagator may consist of a pair of any charged particle and its antiparticle (left half of the figure), but muon and tauon loops cannot produce  $H_e$  particles (right half) — only  $H_\mu$  and  $H_\tau$  particles, respectively.

The Higgs effect (delay with accompanying drift of the signal) is expected to be most pronounced in the Van Allen belts with their accumulation of free protons and electrons.

The strength of the Higgs particle’s interaction with the electron and the up and down quarks is proportional to the mass of these particles [1]. Therefore, the free protons, each one containing three comparatively heavy quarks, are expected to contribute most to the Higgs effect.

Knowing the trajectories of the spacecraft, the time of day when they were nearest to the earth (at perigee), and the frequencies they used for radio communication, it should be fairly easy to check if the flyby anomaly might be related to the direction of motion of the Van Allen belts and the rotation of the ionosphere.

Also, a simple experiment should reveal the existence of the Higgs delay if it exists and is large enough to be observable. For instance, let a satellite transmit four signals — on frequencies 2.0, 2.3, 2.6, and 2.9 GHz, say — at regular intervals and with constant time difference (maybe one millisecond) between the signals. By measuring the corresponding time differences when the signals reach the receiving radio station, it should be possible to detect an “anomalous”

delay of the signals when the satellite passes through or above the Van Allen belts.

### 3.7 The Pioneer anomaly

The Higgs delay assumed to be responsible for the flyby anomaly should cause an effect similar to the so-called Pioneer anomaly [24], which puzzled physicist for twenty years.

Pioneer 10 was launched in 1972 and Pioneer 11 in 1973. When the two spacecraft — after fulfilling their main mission: encounters with Jupiter and Saturn — were leaving the solar system in the early 1980s, measurements indicated that they were slightly less far from the sun and the earth than calculations suggested they should be. This discrepancy between theory and observation seemed to be caused by a mysterious acceleration of the spacecraft toward the sun.

Although a recent study has concluded that the anomalous acceleration of the Pioneer 10 and 11 spacecraft is caused by “anisotropic emission of thermal radiation off the vehicles” [25], it does not exclude that a small part of the anomaly might be due to the appearance of  $H_e$  particles, which cause a small additional delay of the radio signals as they travel through the interplanetary plasma.

Pioneer 10 and 11 transmitted on frequency 2.29 GHz [24], only 21 % below the 2.90 GHz corresponding to the  $H_e$  mass. The measuring systems were calibrated when the spacecraft were in the vicinity of the earth. Due to the unrecognized Higgs delay, the radio signals traveled slightly slower than they were believed to do. Therefore, as the spacecraft approached the outer edge of the solar system and the plasma became thinner, signal speed increased more than it was believed to do — that is, more than it would have increased if the delay only had been caused by absorption and reemission of photons in the signal. The result was that the signals arrived earlier than anticipated, and the spacecraft appeared to be nearer to the sun than they actually were.

p. 4

## 4 Conclusions

By applying the principle of maximum simplicity to the standard model (SM), one arrives at kind of “maximally simple model (MxSM)” based on the finite-QED hypothesis of Johnson, Baker, and Willey [3]. A straightforward interpretation of the Feynman graphs further suggests that the mass-generating so-called Higgs mechanism, in addition to producing the weak masses of the  $Z$  and  $W$  bosons, gives small weak contributions to the electromagnetically generated masses of the electron, which comes in three mass states: the ordinary electron ( $e$ ), the heavy muon ( $\mu$ ), and the superheavy tauon ( $\tau$ ).

It appears that the existence of the light Higgs particle that generates the fermionic weak mass components can explain several observations in physics that

would otherwise require introduction of some sort of “new physics” of unknown nature.

## References

- [1] M. Veltman, *Diagrammatica: The Path to Feynman Diagrams* (Cambridge University Press, 1994), pp. 269–271.
- [2] J. D. Bjorken and S. D. Drell, *Relativistic Quantum Mechanics* (McGraw-Hill, New York, 1964) pp. 162–163.
- [3] K. Johnson, M. Baker, and R. Willey, *Self-Energy of the Electron*, Phys. Rev. **136**, B1111 (1964).
- [4] J. D. Bjorken and S. D. Drell, *Relativistic Quantum Fields* (McGraw-Hill, New York, 1965) pp. 94–96.
- [5] P. D. B. Collins, A. D. Martin, and E. J. Squires, *Particle Physics and Cosmology* (John Wiley & Sons, 1989), p. 98.
- [6] *Dictionary of Physics*, 6th ed. (Oxford University Press, 2009).
- [7] Jeffrey W. Brosius, Adrian N. Daw, and D. M. Rabin, The Astrophysical Journal, 790:112, 2014 August 1.
- [8] P. D. B. Collins, A. D. Martin, and E. J. Squires, *Particle Physics and Cosmology* (John Wiley & Sons, 1989), p. 452.
- [9] J. Jenkins *et al.*, *Additional experimental evidence for a solar influence on nuclear decay rates*, Astroparticle Physics **37**, 81 (2012).
- [10] J. Jenkins, *Jere Jenkins’s articles on arXiv*, arxiv.org/a/jenkins.j\_1.atom.
- [11] E. Fischbach, J. H. Jenkins, and P. A. Sturrock, *Evidence for time-varying nuclear decay rates: experimental results and their implications for new physics*, arxiv.org/abs/1106.1470 (2011).
- [12] Davide Castelvechi, *Radioactive decay rates can change*, November 22nd, 2008, <http://dinosaurc14ages.com/changedecay.htm>.
- [13] A. T. Yue *et al.*, *Improved Determination of the Neutron Lifetime*, Phys. Rev. Lett. **111**, 222501 (2013).
- [14] J. Christopher Howk, Nicolas Lehner, Brian D. Fields, and Grant J. Mathews, *Observation of interstellar lithium in the low-metallicity Small Magellanic Cloud*, Nature **489**, 121 (2012).
- [15] J. D. Cockcroft and E. T. S. Walton, *Disintegration of Lithium by Swift Protons*, Nature **129**, 649 (1932).
- [16] *The Penguin Dictionary of Physics*, 3rd ed. (Market House Books, 2000).

- [17] M. Passera, W. J. Marciano, and A. Sirlin, *The muon  $g - 2$  and the bounds on the Higgs boson mass*, Phys. Rev. D **78**, 013009 (2008).
- [18] *CODATA recommended values of the physical constants: 2010*, Rev. Mod. Phys. **84**, 1527 (2012), p. 1588.
- [19] D. Hanneke, S. Fogwell, and G. Gabrielse, *New Measurement of the Electron Magnetic Moment and the Fine Structure Constant*, Phys. Rev. Lett. **100**, 120801 (2008).
- [20] J. T. Londergan, *Nucleon resonances and quark structure*, Int. J. Mod. Phys. E **18**, 1135 (2009).
- [21] W. Greiner, S. Schramm, and E. Stein, *Quantum Chromodynamics*, 2nd ed. (Springer, 2002), pp. 150–151.
- [22] Randolph Pohl *et al.*, *The size of the proton*, Nature **466**, 213 (2010).
- [23] Evgeny Epelbaum *et al.*, *Structure and Rotations of the Hoyle State*, Phys. Rev. Lett. **109**, 252501 (2012).
- [24] John D. Anderson, Philip A. Laing, Eunice L. Lau, Anthony S. Liu, Michael Martin Nieto, and Slava G. Turyshev, *Study of the anomalous acceleration of Pioneer 10 and 11*, Phys. Rev. D **65**, 082004 (2002).
- [25] Slava G. Turyshev, Viktor T. Toth, Gary Kinsella, Siu-Chun Lee, Shing M. Lok, Jordan Ellis, *Support for the thermal origin of the Pioneer anomaly*, Phys. Rev. Lett. **108**, 241101 (2012).